Oncogene (2017) **36**, 3168–3177

www.nature.com/onc

ORIGINAL ARTICLE

The primacy of *NF1* loss as the driver of tumorigenesis in neurofibromatosis type 1-associated plexiform neurofibromas

A Pemov[1], H Li[2], R Patidar[3], NF Hansen[4], S Sindiri[3], SW Hartley[5], JS Wei[3], A Elkahloun[4], SC Chandrasekharappa[4], NISC Comparative Sequencing Program[6], JF Boland[7], S Bass[7], NCI DCEG Cancer Genomics Research Laboratory[7], JC Mullikin[4,6], J Khan[3], BC Widemann[8], MR Wallace[2] and DR Stewart[1]

Neurofibromatosis type 1 (NF1) is a common tumor-predisposition disorder due to germline mutations in the tumor suppressor gene *NF1*. A virtually pathognomonic finding of NF1 is the plexiform neurofibroma (PN), a benign, likely congenital tumor that arises from bi-allelic inactivation of *NF1*. PN can undergo transformation to a malignant peripheral nerve sheath tumor, an aggressive soft-tissue sarcoma. To better understand the non-*NF1* genetic contributions to PN pathogenesis, we performed whole-exome sequencing, RNASeq profiling and genome-wide copy-number determination for 23 low-passage Schwann cell cultures established from surgical PN material with matching germline DNA. All resected tumors were derived from routine debulking surgeries. None of the tumors were considered at risk for malignant transformation at the time; for example, there was no pain or rapid growth. Deep (~500X) *NF1* exon sequencing was also conducted on tumor DNA. Non-*NF1* somatic mutation verification was performed using the Ampliseq/IonTorrent platform. We identified 100% of the germline *NF1* mutations and found somatic *NF1* inactivation in 74% of the PN. One individual with three PNs had different *NF1* somatic mutations in each tumor. The median number of somatic mutations per sample, including *NF1*, was one (range 0–8). *NF1* was the only gene that was recurrently somatically inactivated in multiple tumors. Gene Set Enrichment Analysis of transcriptome-wide tumor RNA sequencing identified five significant (FDR < 0.01) and seven trending ($0.01 \leqslant$ FDR < 0.02) gene sets related to DNA replication, telomere maintenance and elongation, cell cycle progression, signal transduction and cell proliferation. We found no recurrent non-*NF1* locus copy-number variation in PN. This is the first multi-sample whole-exome and whole-transcriptome sequencing study of NF1-associated PN. Taken together with concurrent copy-number data, our comprehensive genetic analysis reveals the primacy of *NF1* loss as the driver of PN tumorigenesis.

Oncogene (2017) **36,** 3168–3177; doi:10.1038/onc.2016.464; published online 9 January 2017

INTRODUCTION

Neurofibromatosis type 1 (NF1) is a common (1/3,000), autosomal dominant, fully penetrant neurocutaneous tumor-predisposition disorder that is caused by mutations in the tumor suppressor gene *NF1*, located on chromosome 17q11.2.[1] It is diagnosed using well-established clinical criteria[2] that emphasize specific hallmark features including café-au-lait macules, intertriginous freckling, neurofibromas, optic pathway gliomas, and specific bone dysplasias. A virtually pathognomonic finding of NF1 is the plexiform neurofibroma (PN), an often-congenital neurofibroma that affects 30% (when defined clinically[3]) to 56% (when identified by imaging[4]) of people with the disorder. Malignant peripheral nerve sheath tumors (MPNSTs) are aggressive soft-tissue sarcomas with limited therapeutic options that frequently arise from PN. People with NF1 have a lifetime risk of about 15% to develop MPNST.[5,6] PNs arise from within spinal, cranial and peripheral nerves and typically involve multiple nerve roots or the length of a single nerve and may occur anywhere, although there is a predilection for neck and trunk, at least in those patients enrolling in treatment trials.[7] The growth of PN tends to track with that of the individual, tapering off in late adolescence, although in some patients the growth rate is unpredictable and can be very disfiguring, especially early in childhood.[8] Some PNs may not be diagnosed until adulthood, and thus the timing of the origin is unknown. Prognostication of PN growth for a specific patient is difficult, and no therapies, other than surgery, are effective, despite a number of trials testing novel agents.[9,10] Clinically, in addition to their contribution to MPNST pathogenesis, PNs are a significant cause of morbidity due to their propensity for local invasion, bone erosion, organ compression, chronic pain and untoward esthetics.

Histologically, PN are similar to solitary neurofibromas and are composed of myxoid stroma and a cellular component. The cellular element is heterogeneous and complex and consists primarily of S-100-positive Schwann cells (60–80%)[11] but also fibroblasts, endothelial cells, perineurial cells, smooth muscle cells, mast cells, residual interspersed axons and pericytes.[12] In neurofibromas, the Schwann cell is the primary neoplastic cell and is the only cell to harbor a 'second hit' in the *NF1* gene.[13,14]

[1]Clinical Genetics Branch, Division of Cancer Epidemiology and Genetics, National Cancer Institute, Rockville, MD, USA; [2]Department of Molecular Genetics and Microbiology, UF Genetics Institute, UF Health Cancer Center, University of Florida, Gainesville, FL, USA; [3]Genetics Branch, Center for Cancer Research, National Cancer Institute, Bethesda, MD, USA; [4]Cancer Genetics and Comparative Genomics Branch, National Human Genome Research Institute, Rockville, MD, USA; [5]Human Genetics Program, Division of Cancer Epidemiology and Genetics, National Cancer Institute, Rockville, MD, USA; [6]NIH Intramural Sequencing Center, National Human Genome Research Institute, Rockville, MD, USA; [7]Cancer Genomics Research Laboratory, Division of Cancer Epidemiology and Genetics, National Cancer Institute, Rockville, MD, USA and [8]Pediatric Oncology Branch, Center for Cancer Research, National Cancer Institute, Bethesda, MD, USA. Correspondence: Dr DR Stewart, Division of Cancer Epidemiology and Genetics, National Cancer Institute, 9609 Medical Center Drive Rm 6E450, Bethesda, MD 20892, USA.
E-mail: drstewart@mail.nih.gov
Received 23 October 2015; revised 2 November 2016; accepted 5 November 2016; published online 9 January 2017

Although it is clear that *NF1* nullizygosity in a subset of Schwann cells is critical for PN development, we have limited or conflicting understanding of the other genetic factors that contribute to PN tumorigenesis. From family studies, we know that PN burden is heritable[15] and not associated with the type of germline *NF1* mutation[16] or wildtype *NF1* allele.[15] The noncoding RNA *ANRIL* has been proposed as a modifier of PN burden.[17] MPNSTs, unlike PNs, are complex, genetically rearranged tumors that harbor somatic mutations or copy-number changes in *TP53*, *CDKN2A/B*, *EGFR*, *mTOR*, *ERBB2*, *KIT*, *HGF*, *MET*, *SUZ12* and *PDGFRA*.[18–21] One microarray study found the only recurrent somatic alteration in PN were deletions of the *CDKN2A/B-ANRIL* locus at 9p21.3 in 6/22 tumors.[17] Activation of the WNT signaling pathway may also be a feature of PN and MPNST tumorigenesis.[19] We are aware of only one publication that exome-sequenced a single PN as part of its malignant transformation to a MPNST.[22]

To better understand the non-*NF1* genetic contributions to PN pathogenesis, we performed whole-exome sequencing, RNASeq profiling and copy-number determination for 23 low-passage Schwann cell cultures established from surgical PN material.

RESULTS

Whole exome-sequencing (WES) of 23 NF1-associated PNs with matching germline DNA resulted in high confidence genotypes (most probable genotype quality score > 10) in ~90% of target nucleotides. The average depth of coverage was 55X and 63X for germline and tumor DNA, respectively (Supplementary Table S1).

Identification of germline and somatic mutations in *NF1*

In addition to WES, we performed deep sequencing (~500X) of the coding part of *NF1* in all PNs on the IonTorrent platform. We identified germline *NF1* mutations in 100% of the 23 samples (Figure 1, Supplementary Table S2A). Note that two of the samples were tumors from monozygous twins (PN23 and PN24) and three samples were independent tumors from the same patient obtained at different times (PN25, PN26 and PN28), for a total of 21 independent *NF1* germline mutations. Germline mutation type in decreasing order of frequency were: frame-shifting indels (38%), nonsense (33%), splice-site (14%), missense (10%) and a single total gene deletion (5%; Table 1). All mutations except two were truncating, affected splice-sites and/or were reported in HGMD as pathogenic. Of the two exceptions, the missense mutation in PN11 (exon21, c.2542G > T, G848W) results in substitution of glycine, the smallest aliphatic amino acid, by tryptophan, a bulky aromatic compound, likely leading to significant modification or inactivation of the protein function. It is also not observed in the ExAC reference of 61,000 exomes. The second exception was a silent substitution in PN19 (exon31, c.4269G > A, p.K1423K). This synonymous missense mutation is not observed in ExAC and results in a cryptic splice site that results in an in-frame loss of 27 bp of coding sequence. Therefore we consider the two 'exceptions' to also be pathogenic germline mutations.

We identified somatic *NF1* mutations in 74% of the 23 tumors (Table 1 and Supplementary Table S2B). There were 7 (30%) large deletions, 6 (26%) nonsense and 2 (9%) frame-shifting variants. We found two somatic *NF1* missense mutations (R997K in PN9, and G2481E in PN11) that appear pathogenic because they affect conserved residues and are *de novo* hits in the *NF1* gene with no other apparent pathogenic somatic mutation. Both variants have CADD scores > 20 and thus are predicted to be in the top 1% of deleteriousness.[23] Neither of these somatic missense mutations were previously reported in HGMD, COSMIC or ExAC. R997K in PN9 was detected by both WES and IonTorrent sequencing and appears to be present in the majority of tumor cells, while G2481E in PN11 was identified by IonTorrent only and is present only in a small number of cells. Two tumors (PN21 and PN26) showed two

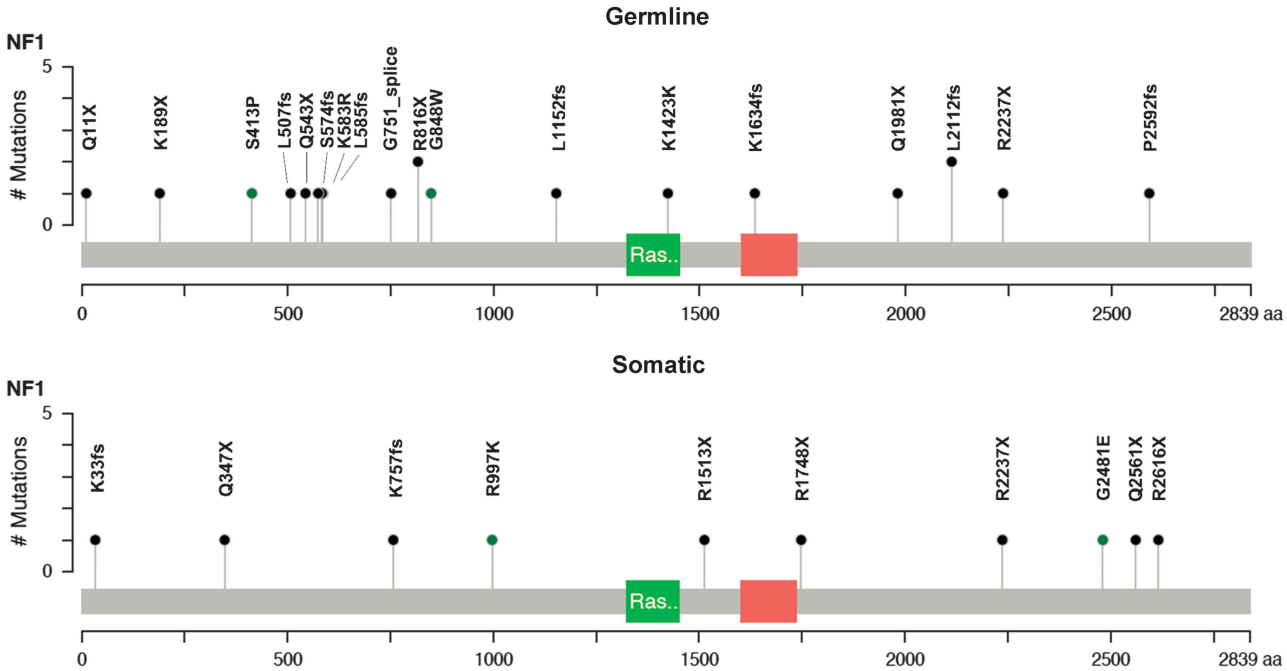

Figure 1. Distribution of germline (upper panel) and somatic (lower panel) *NF1* mutations among 23 plexiform neurofibromas. Black and green dots represent truncating (nonsense, frame-shifting indels and splice-site substitutions) and missense mutations, respectively. Green and red rectangles represent the RAS-GAP and CRAL/TRIO (SEC14-like) domains, respectively. Note that germline substitutions K583R and K1423K result in splicing defects and therefore depicted with black dots. The germline nonsense mutation R816X was found in two unrelated individuals, and the germline frame-shifting mutation L2112fs was found in monozygotic twins and was counted for both individuals. Large deletions are not shown on the diagram (for details see Supplementary Tables S2A and B).

somatic mutations each (a missense variant accompanied by either a nonsense (PN21) or frameshifting (PN26) variant), that were identified by IonTorrent deep sequencing but not WES.

All frame-shifting small indels detected in germline and tumor DNA were novel, whereas the majority of nonsense, and splice-site point substitutions had been previously reported. Germline and somatic missense mutations were both previously reported and novel. Importantly, in the patient with the three different PN (PN25, PN26, PN28), three different second hits in *NF1* occurred, suggesting a stochastic random deactivation of the normal copy of the gene, as first proposed by Colman *et al*.[24]

NF1 expression in PN and normal schwann cells

Compared with normal Schwann cells (100%), median *NF1* expression in PN was 53% (range: 16–107%; Figure 2). Samples with lower expression values of *NF1* (lower half of samples in Figure 2a) had a higher number of total/partial gene deletions (6 vs 1), as well as frame-shifting indels (8 vs 5) and nonsense mutations (7 vs 5) compared with the samples with higher expression values of the gene. This observation is consistent with the previous findings that nonsense and frame-shifting mutations may trigger some degree of nonsense mediated decay of RNA molecules with multiple stop codons. Interestingly, samples without second hits were found in the upper half of the expression value distribution (Figure 2).

NF1 as the sole driver in pathogenesis of plexiform neurofibromas

Besides *NF1*, we identified 26 high-confidence somatic mutations; 19 (73%) were non-synonymous and 15 (58%) were potentially damaging (Table 2; Supplementary Table S3). Three of the 15 potentially damaging variants were in recognized cancer genes (*BRCA1*, *FGFR1* and *RNF43*). Three variants (*FGFR1*, *RNF43* and *ELMOD3*) have been observed a total of four times in The Cancer Genome Atlas. None of the 26 non-*NF1* somatic mutations have been reported in other NF1-associated tumors, including lower-grade glioma,[25] soft-tissue sarcoma[26] or glioblastoma[27,28] sequencing projects. *NF1* was the only gene that was somatically mutated in multiple samples. The lack of recurrent, deleterious mutations in biologically plausible genes suggests that these variants are 'passengers' and not primary drivers of plexiform neurofibromagenesis. The distribution of these 15 non-*NF1* putatively-damaging somatic mutations among the 23 PN tumors is shown in Table 3; only five tumors (22%) had potentially damaging somatic mutations outside of the *NF1* locus. The median number of somatic mutations per sample (including mutations in *NF1*) was one (range 0–8). Interestingly, only six out of these 15 genes were expressed in the tumors or normal Schwann cells as determined by RNAseq analysis, suggesting that only a minor proportion of mutations could potentially play a role in tumor phenotype.

RNA sequencing-based PN transcriptome analysis reveals perturbed expression of DNA replication, cell cycle and telomere maintenance pathways

We analyzed expression of 11293 genes in PNs and cultured normal (wild-type) Schwann cells with the Molecular Signature Database and identified five significantly-altered gene sets (FDR < 0.01) and seven trending ($0.01 \leqslant$ FDR < 0.02) sets in the 'Curated', 'Hallmark', 'Gene Ontology' and 'Oncogenic Signatures' collections (Supplementary Table S4; Figure 3).

Table 1. Types and number (percentage) of germline and somatic *NF1* mutations in 21 germline and 23 PN samples

	Nonsense	*Frameshifting*	*In-frame*	*Missense*	*Splice*	*Total or partial NF1 deletion or copy-neutral LOH*	*Not detected*	*Total*
Germline	7 (33)	8 (38)	0 (0)	2 (10)	3 (14)	1 (5)	0 (0)	21 (100)
Somatic	6 (26)	2 (9)	0 (0)	2 (9)	0 (0)	7 (30)	6 (26)	23 (100)

a

Sample_Cell ID	Germline/Somatic *NF1* mutation	Normalized expression (%)
Normal Schwann cells	NA/NA	100
PN12_pNF00.8	Stop/Not detected	107
PN13_pNF01.1	Splicing/Frameshift	105
PN29_pNF99.5	Missense/Not detected	94
PN14_pNF04.5	Stop/PGD	89
PN19_pNF03.3	Splicing/Not detected	87
PN11_pNF06.2A	Missense/Missense	73
PN26_pNF05.10	Frameshift/Frameshift	63
PN24_pNF05.4	Frameshift/Not detected	62
PN22_pNF04.8	Frameshift/Not detected	60
PN9_pNF01.2B	Stop/Missense	56
PN21_pNF04.6	Stop/Stop	54
PN16_pNF00.6	TGD/Not detected	53
PN27_pNF08.1	Frameshift/CN-LOH	51
PN17_pNF01.3	Stop/TGD	49
PN23_pNF05.3	Frameshift/Stop	44
PN8_pNF04.4	Stop/PGD	39
PN28_pNF09.3	Frameshift/Frameshift	38
PN15_pNF05.8	Frameshift/Stop	38
PN7_pNF03.4	Splicing/Stop	26
PN10_pNF95.6	Stop/Stop	26
PN25_pNF05.5	Frameshift/TGD	22
PN5_pNF95.11b	Frameshift/TGD	19
PN6_pNF00.13	Frameshift/TGD	16

b

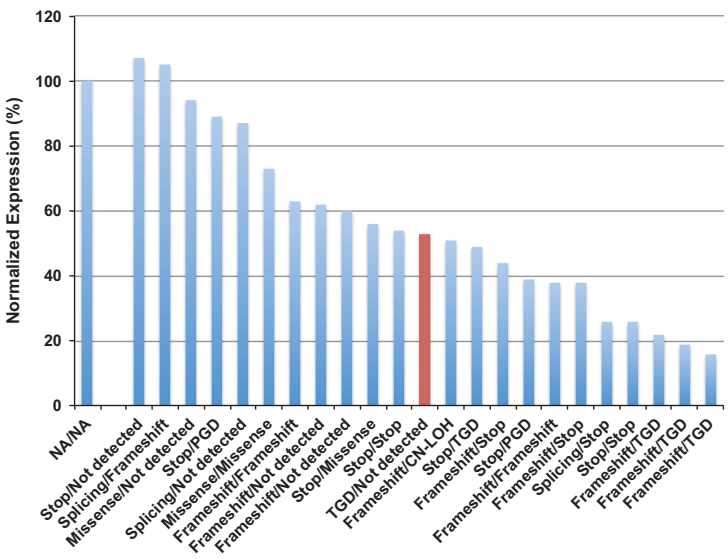

Figure 2. *NF1* expression in PN and normal Schwann cells. (**a**) Table shows sample or cell identification, type of the germline and somatic mutations in *NF1* and expression values compared with that in normal Schwann cells (%). The PN sample with the median expression value (53%) is highlighted with red font. CN-LOH: Copy Neutral Loss Of Heterozygosity; PGD: Partial Gene Deletion; TGD: Total Gene Deletion. (**b**) Bar graph of the values shown in (**a**). Sample with the median expression value (53%) is shown in red. NA, not applicable.

Table 2. Non-*NF1* mutations identified by WES and verified by AmpliSeq/IonTorrent

Gene ID	*Chr*	*Position*	*Ref*	*Alt*	*Mutation type*	*ExAC frequency*	*Mutation deleteriousness*	*Gene expression*	*Sample ID*	*Cell ID*
TNFRSF11B	8	119 936 782	A	G	Missense	0	Tolerated	Not expressed	PN6	pNF00.13
SLC25A5	X	118 605 018	A	C	Synonymous	4.47E-04	Tolerated	Expressed	PN9	pNF01.2B
KIF2B	17	51 900 433	C	G	Synonymous	5.53E-04	Tolerated	Not expressed	PN27	pNF08.1
PLEKHG4	16	67 322 137	G	T	Synonymous	0	Tolerated	Expressed	PN26	pNF05.10
TENM1	X	123 654 614	G	T	Synonymous	0	Tolerated	Not expressed	PN22	pNF04.8
LRIG3	**12**	**59 284 551**	**G**	**T**	**Synonymous**	**0.029**	**Tolerated**	**Expressed**	**PN9**	**pNF01.2B**
PADI1	1	17 531 755	A	G	Missense	1.55E-04	Tolerated	Not expressed	PN9	pNF01.2B
FREM1	9	14 857 623	G	A	Synonymous	0	Tolerated	Not expressed	PN9	pNF01.2B
OR4S1	11	48 328 256	C	T	Missense	2.28E-04	Tolerated	Not expressed	PN26	pNF05.10
IL7R	**5**	**35 873 605**	**G**	**A**	**Synonymous**	**0.012**	**Tolerated**	**Expressed**	**PN9**	**pNF01.2B**
OTX2	14	57 268 991	G	A	Missense	0	Tolerated	Not expressed	PN28	pNF09.3
USP18	22	18 652 695	C	T	Missense	3.02E-04	Damaging	Expressed	PN9	pNF01.2B
FGFR1	**8**	**38 271 301**	**G**	**A**	**Missense**	**3.83E-03**	**Damaging**	**Expressed**	**PN9**	**pNF01.2B**
BRCA1	**17**	**41 244 982**	**A**	**G**	**Missense**	**1.51E-03**	**Damaging**	**Expressed**	**PN27**	**pNF08.1**
WDHD1	14	55 408 293	T	A	Missense	0	Damaging	Expressed	PN26	pNF05.10
LAMA5	20	60 899 525	C	T	Missense	4.91E-05	Damaging	Not expressed	PN9	pNF01.2B
ADAM11	17	42 851 945	C	T	Missense	3.90E-04	Damaging	Not expressed	PN27	pNF08.1
ABHD15	17	27 889 968	C	T	Missense	6.51E-05	Damaging	Expressed	PN6	pNF00.13
ELMOD3	2	85 598 245	G	A	Missense	5.77E-04	Damaging	Expressed	PN9	pNF01.2B
DNAH17	17	76 455 168	G	A	Missense	1.38E-03	Damaging	Not expressed	PN27	pNF08.1
TGM4	3	44 948 656	C	T	Missense	9.76E-05	Damaging	Not expressed	PN9	pNF01.2B
RNF43	**17**	**56 435 552**	**G**	**A**	**Missense**	**2.42E-03**	**Damaging**	**Not expressed**	**PN9**	**pNF01.2B**
UNC5D	8	35 579 857	A	T	Missense	0	Damaging	Not expressed	PN9	pNF01.2B
CNTN2	1	205 031 633	G	A	Missense	0	Damaging	Not expressed	PN26	pNF05.10
GREB1	2	11 767 136	C	T	Missense	1.55E-04	Damaging	Not expressed	PN26	pNF05.10
POU4F2	4	147 561 811	G	T	Stop_gained	0	Damaging	Not expressed	PN13	pNF01.1

Gene name, chromosomal location (hg19), reference and alternative alleles, type of mutation, frequency of variant allele in ExAC db, mutation deleteriousness as predicted by PolyPhen, SIFT and CADD (mutation was considered damaging if it was classified as probably or possibly damaging by PolyPhen, OR deleterious by SIFT, OR its CADD score was above 20), the status of the gene expression in PNs and normal Schwann cells as measured by total transcriptome sequencing and sample and cell IDs are shown. Known cancer genes are shown in bold font.

Eight gene sets were up-regulated and four gene-sets were down-regulated in PN compared with normal Schwann cells. There were 300 genes in the 12 sets that contributed to the enrichment score (the leading-edge genes), and 60 genes were found in at least two different gene sets (Supplementary Table S4). Plotting expression of these genes in tumors vs normal Schwann cells revealed that 52 of them found in up-regulated sets were moderately overexpressed and eight genes found in down-regulated sets were under-expressed in tumors (Figure 4).

Copy-number analysis identifies no recurrent non-*NF1* copy number variations

Remarkably, we did not identify a single significant recurrent copy number variation (CNV) outside of the *NF1* locus by Nexus analysis. We found copy-neutral loss of heterozygosity (LOH) affecting the entire q-arm of chromosome 17 in a single tumor (PN27) by both ASCAT and Nexus consistent with mitotic recombination; six additional smaller partial or total *NF1* deletions were identified with the Nexus algorithm only (Supplementary Table S5). The size of the deletions ranged from 66 kb (ten exons in the middle of the *NF1* gene) to over 24 Mb (the entire 17q-arm). None of the somatic deletions extended into the 17p arm, where *TP53* resides, however, in four tumors the deletion also comprised entire *SUZ12*, which is frequently inactivated in MPNSTs.

DISCUSSION

This study is the first multi-sample whole-exome and whole transcriptome sequencing analysis of NF1-associated PN. Previous work in PN has focused on their cell of origin and micro-environment,[29] dysregulated pathways,[19] and timing of development.[30] One study of WES of PN, MPNST and associated metastases samples collected from a single patient over 14 years found a very limited number of mutations in the PN samples, none of which overlapped with our findings. No copy-number changes were detected in three PN samples from the single patient.[22] Cytogenetic abnormalities have been identified more frequently in cells derived from PN than from dermal neurofibromas, however no consistent chromosomal regions with abnormal karyotypes have been identified in PN.[31] From this work, we establish that the overall exome mutation rate in PN is very low and comparable with pediatric malignancies. The somatic variants (other than *NF1*) that were confirmed on a second platform appeared in one sample only and most were not predicted to be significantly pathogenic. Furthermore, the majority were found in genes that were not expressed in the tumors or normal Schwann cells. We found no recurrent copy-number variation in PN outside the *NF1* locus. Despite the low number of somatic mutations and CNVs in PN, we observed that expression of 300 genes in several key cellular processes, such as DNA replication initiation and strand elongation, cell cycle progression and telomere maintenance and extension, was perturbed. Taken together, our comprehensive genetic analysis reveals the primacy of *NF1* loss as the driver of plexiform neurofibroma tumorigenesis.

We identified germline *NF1* mutations in 100% of the samples and a somatic *NF1* 'second hit' in 74% of PN, a rate that is comparable with previous studies.[32] We deep-sequenced (500X) all *NF1* exons and intron-exon boundaries in the PN and therefore it is unlikely that we missed any mutations or short indels in those regions. We also carefully examined *NF1* RNA transcripts from PN for evidence of aberrantly spliced species, which may have suggested the presence of deep intronic mutations, but did not find any (data not shown). We acknowledge that the SNP arrays we used have limited resolution and would likely fail to detect

Table 3. Distribution of 15 non-*NF1* potentially damaging mutations as well as germline and somatic hits in *NF1* among 23 PN

Sample ID	*Age at surgery*	*NF1-germline*	*NF1-somatic*	*POU4F2*	*GREB1*	*CNTN2*	*UNC5D*	*RNF43*	*TGM4*	*DNAH17*	*ELMOD3*	*ADAM11*	*ABHD15*	*LAMA5*	*WDHD1*	*BRCA1*	*FGFR1*	*USP18*
PN9	42	Found	Found				Found	Found	Found		Found			Found			Found	Found
PN26	31	Found	Found		Found	Found									Found			
PN27	16	Found	Found							Found		Found				Found		
PN6	15	Found	Found										Found					
PN13	34	Found	Found	Found														
PN28	36	Found	Found															
PN5	20	Found	Found															
PN7	22	Found	Found															
PN8	35	Found	Found															
PN10	3	Found	Found															
PN11	69	Found	Found															
PN14	39	Found	Found															
PN15	43	Found	Found															
PN17	58	Found	Found															
PN21	9	Found	Found															
PN23	21	Found	Found															
PN25	31	Found	Found															
PN12	24	Found																
PN16	23	Found																
PN19	5	Found																
PN22	27	Found																
PN24	21	Found																
PN29	5	Found																

Names of genes that were not expressed in the tumors and normal Schwann cells are indicated with gray fill. Known cancer genes are shown in red font. The presence of mutations in genes is indicated with green fill.

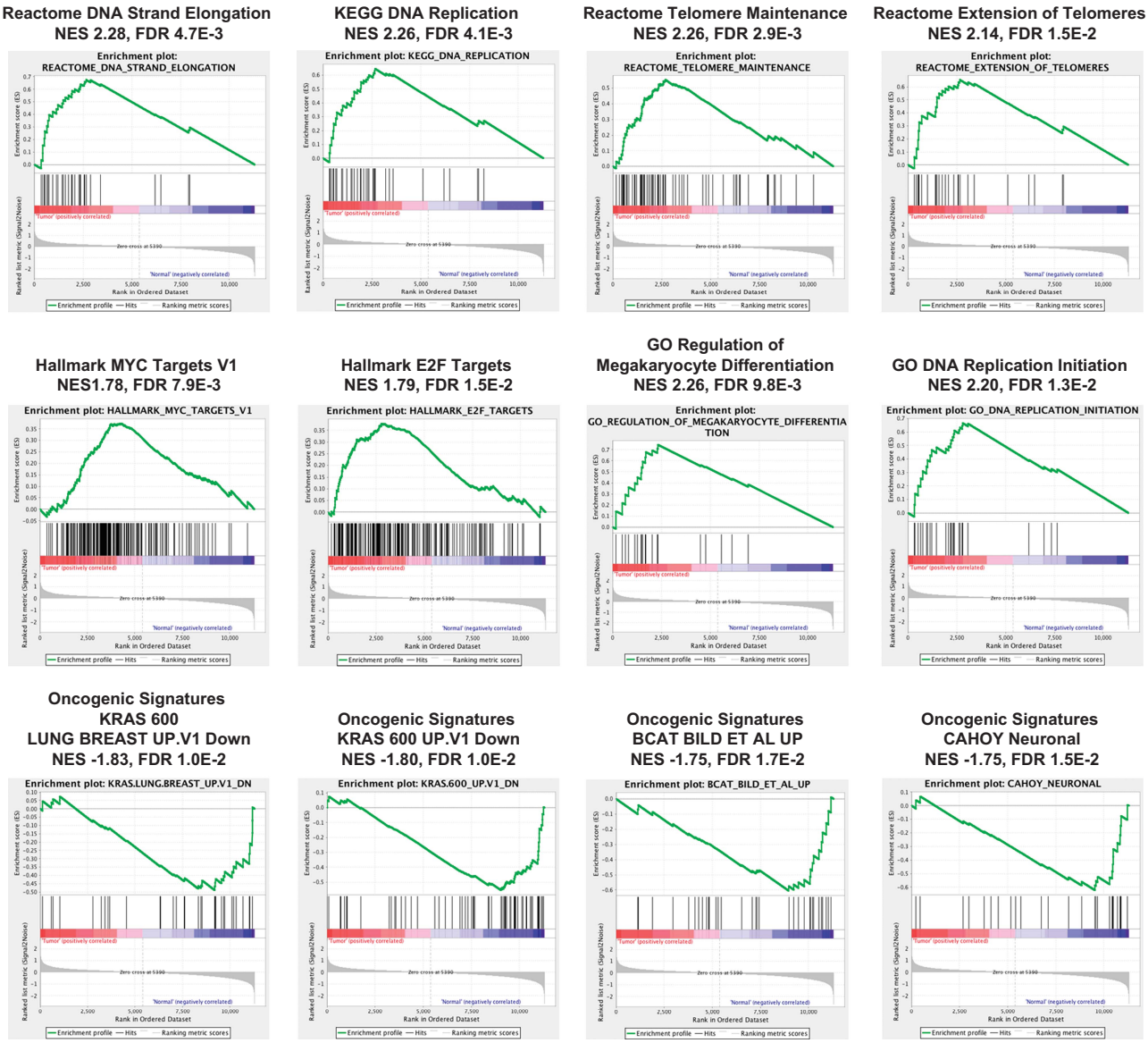

Figure 3. Gene Set Enrichment Analysis of genome-wide expression in PN. Enrichment plots of five significant and seven trending sets of genes involved in DNA replication initiation and strand elongation, telomere maintenance and extension, cell proliferation and differentiation, as well as gene sets comprising targets of MYC and E2F, and down-regulated by activated KRAS. FDR, false discovery rate; NES, normalized enrichment score.

medium-sized (100–1000 bp) deletions; however, such deletions are also difficult to identify by NGS approaches. Furthermore, samples with undetected second hits had relatively high levels of *NF1* expression, suggesting that these samples contain a relatively smaller ratio of tumor cells. We posit that the samples with undetected second hits harbor deep intronic and/or medium-sized deletions and occur in PNs with a relatively low proportion of $NF1^{-/-}$ Schwann cells. The spectrum and distribution of *NF1* LOH events and discrete mutations in PN from our study was also comparable with previous work.[32] Independent somatic mutations in *NF1* have been reported in individuals with two PN.[33] We found non-*NF1* somatic mutations at a very low frequency (Tables 2 and 3), as predicted for a congenital tumor such as a PN. Given the low mutation rate, we cast a broad net to identify somatic variants but applied a rigorous filtering (overlap) scheme to reduce the number of false positives. We acknowledge that our filtering strategy might increase the false-negative rate and we acknowledge that the modest number of samples limits the power.

The non-*NF1* somatic mutations identified (Tables 2 and 3) appear in a fraction of the reads, suggesting that the cell harboring the mutation is a clonal derivative. Most of these variants are not pathogenic, as predicted by a variety of bioinformatics methods, and do not reside in known cancer pathways. None of the non-synonymous somatic variants in *BRCA1, FGFR1* and *RNF43* (known cancer genes) from two tumors (Table 2 and Supplementary Table S3) were present in the COSMIC database. The rs80356892 missense variant in *BRCA1* was heterozygous in the germline that became homozygous in the PN due to a large deletion on chromosome 17, which also affected the *NF1* locus. *BRCA1* was modestly expressed in the tumor (Supplementary Table S3). The variant was originally identified in a Japanese patient who developed a breast cancer at age of 54 years,[34] however subsequent multi-center ClinVar review has deemed it benign (ClinVar variant ID # 54604). The NF1 patient harboring this variant has not developed any tumors other than a PN, however she is only in her mid-20s; the histopathology of her

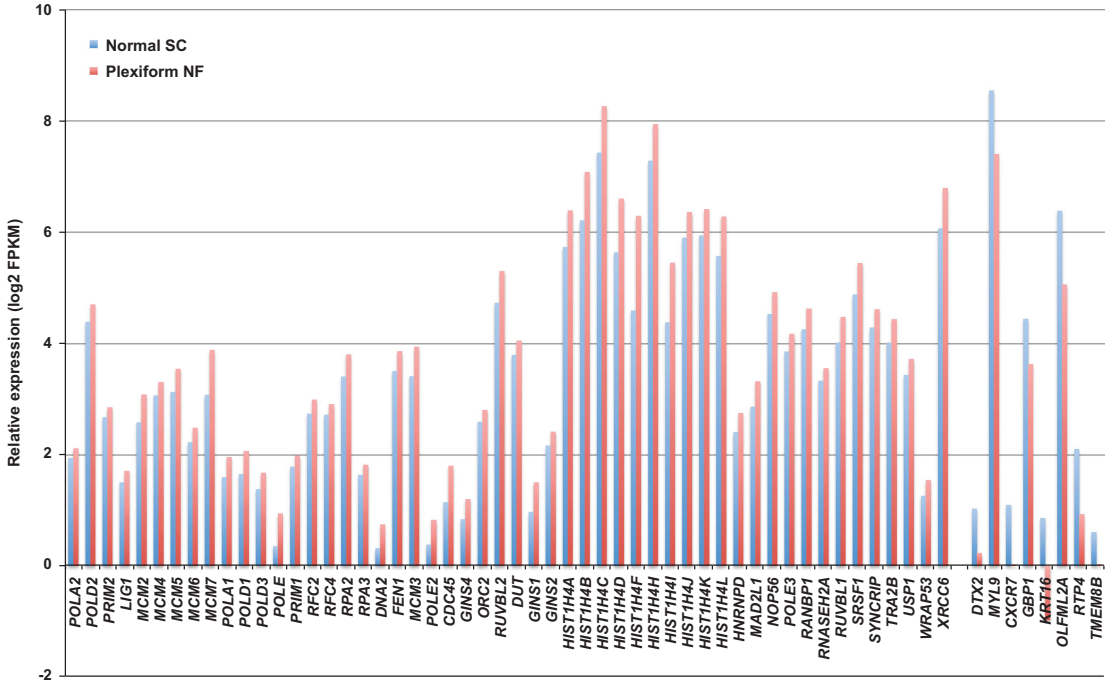

Figure 4. Expression of 60 Gene Set Enrichment Analysis leading-edge genes in PN and normal Schwann cells. Expression values of genes that were found in at least two significant sets are shown. Blue bars represent normal Schwann cells, and red bars represent PN. Fifty-two genes (*POLA2* through *XRCC6)* are up-regulated and eight genes (*DTX2* through *TMEM8B*) are down-regulated in PN compared with normal Schwann cells (SC). Note that raw median expression value of *KRT16* in PN is 0.51, which results in negative value of − 0.97, when log2 transformed.

PN was unremarkable. The missense variant in *RNF43* in tumor PN9 was predicted to be deleterious, however the gene was not expressed in PNs and the variant likely had no effect on the tumor phenotype. The missense *FGFR1* variant in tumor PN9 (P772S) was present in parity with its reference allele (Supplementary Table S3), suggesting that it was acquired by the cell soon after the somatic *NF1* hit (Ref/Alt counts = 1039/956, Supplementary Table S2B). The gene was modestly expressed in the tumor and the mutant allele was expressed at the same rate as the reference one (Supplementary Table S3). *FGFR1* is a tyrosine-protein kinase that plays an essential role in the regulation of embryonic development, cell proliferation, differentiation and migration. It mediates activation of RAS, MAPK1/ERK2, MAPK3/ERK1 and the MAP-kinase signaling pathway, as well as the AKT1 signaling pathway. Although *FGFR1* P772S was reported to be associated with Kallmann syndrome in an earlier paper,[35] its high prevalence in the ExAC database argues (3.83×10^{-3}) against pathogenicity. The PN9 tumor had a relatively loose extra cellular matrix, but was otherwise unremarkable.

Much of the literature on gene expression profiling in NF1 investigates the transition of PN to MPNST.[36,37] There are few investigations comparing PN expression with normal Schwann cells. In the most comprehensive to date study, Miller *et al.*[38] compared primary tissue and primary cell cultures of PN, dermal neurofibroma, and MPNSTs with wild-type Schwann cells using gene expression arrays. They found 2827 distinct transcripts in 1952 unique genes differentially expressed among these groups of samples; dermal neurofibroma and PN did not differ significantly from each other. Unlike previous studies that utilized a microarray approach, we used whole-transcriptome RNA-sequencing data to determine differential expression in PN vs normal Schwann cells. In addition, we used Gene Set Enrichment Analysis, an established analytical method that derives its power by focusing on sets of genes, grouped by their function and biology, rather than employing a single-gene approach, known for having a number of limitations. We found five highly statistically significant (FDR < 0.01) and seven trending ($0.01 \leqslant$ FDR < 0.02) gene sets with known roles in DNA replication, cell proliferation, cell cycle control and telomere maintenance. One of the best-studied consequences of *NF1* inactivation is RAS-mediated hyper-activation of the Ras-MAPK and AKT1-PI3K pathways, which play key roles in cell proliferation and differentiation.[39] The functional connection between *NF1* inactivation and telomere maintenance and elongation and is less studied, however it may provide insights into mechanisms of immortalization and genomic instability in the tumors. Comparison of the leading-edge set of 300 genes with the set of 1952 differentially expressed genes from Miller *et al.*[38] revealed an overlap of 36 genes with a *p*-value of 0.021.

The majority of published investigations on CNV differences in NF1-associated tumors (with paired germline DNA) have been performed on MPNSTs. The few studies that have investigated PNs found a paucity of such changes and a lack of specific recurrent CNVs. Upadhyaya *et al.* is a typical example and studied CNVs using the Affymetrix Array 6.0 chip and found 996 copy differences in 15 MPNSTs and 26 copy differences in 5 PNs (both paired analyses); 17 of these changes were in a single sample.[40] The ratio of gains to losses was 24/2. Except for one overlap on chromosome 4 in two patients, there were no recurring or overlapping CNVs.[40] In our study, we did not find any recurrent CNVs outside the *NF1* locus. We noticed that the majority of large somatic deletions on 17q comprising the *NF1* locus also contained the entire *SUZ12* gene. Currently it's unclear if hemizygous deletion of *SUZ12* confers any advantage in PN-MPNST transformation.

The limited clinical information available on the PNs is included in the Supplementary Clinical Information file. We emphasize that all tumors in this study were asymptomatic and procured from routine debulking surgeries. They were classified as neurofibromas and were not suspected as pre-malignant or malignant lesions; for

example, the tumors were not associated with pain or increased growth. Atypical neurofibroma (ANF) and MPNST often arise within pre-existing PNs[18] and it is difficult to detect these tumors clinically in the early stages. In rare instances, a PN tissue could be intermixed with ANF or MPNST, and when cultured pre-malignant or malignant cells could potentially outgrow the benign ones, however we expect that such scenarios would be relatively infrequent and therefore the effect of such tissue heterogeneity on the results would be limited.

In summary, our data show that initiation of NF1-associated PN, a benign, slowly growing tumor, is driven by somatic inactivation of *NF1*. We observed three independent somatic *NF1* mutations in three PN from the same individual, consistent with a clonal origin. Plexiform neurofibromas harbor a near-zero mutation burden outside of the *NF1* locus, and the genomic architecture of the tumors closely resembles that of a normal diploid cell. It appears that inactivation of *NF1* is sufficient for PN initiation. A series of additional mutations is likely required for subsequent malignant transformation.

MATERIALS AND METHODS

Samples were collected under the IRB-approved protocol ('Genetic Studies of Neurofibromatosis 1' 41–1992) and reviewed by the NIH Office of Human Subjects Research. Twenty-three fresh surgical specimens (2–10 g) were obtained from 21 independent subjects (including one set of identical twins) undergoing PN debulking for cosmetic or functional reasons and not for concern about pain or rapid growth. All non-tumor-appearing tissue was trimmed away; the remaining tissue was fresh frozen and processed using standard methods for formalin fixing/paraffin embedding, DNA extraction, total RNA extraction (Trizol, Invitrogen), and dissociation into single cell suspension for Schwann-enriched culture. Germline DNA was obtained from EDTA-blood samples, buccal swabs, or from fibroblast cultures derived from the tumor cultures.

Culture of schwann cells

Enriching and culturing of $NF1^{-/-}$ Schwann cells from NF1-associated PN and normal human Schwan cells was done as described previously.[41] Cultures always contain at least some fibroblasts, and the Schwann cell component usually senesces by P8-P10, thus passages P4-P6 were used for most studies. Three cultures of normal human Schwann cells purchased from ScienCell Research Laboratories (Carlsbad, CA) were cultured the same way. One sample, PN9, required whole-genome amplification of both somatic and germline DNA.

Whole exome sequencing of matching pairs of tumor and normal DNA

Exome capture of genomic DNA and library preparation for next generation sequencing was done by using Illumina TruSeq V1:32 and TruSeq V2:30 kits (62 Mb), per the manufacturer's instructions on 1 μg of tumor and matching normal genomic DNA. The sequencing was done on the Illumina HiSeq 2,500 system (Illumina, San Diego, CA, USA). Of 44 exomes, the average breadth of coverage was 89% (range 84–92%); the average depth of coverage was 59X (range 34–108X).

RNA extraction, Illumina whole transcriptome sequencing and Gene Set Enrichment Analysis (GSEA)

RNA extraction and Illumina RNA sequencing was done as described previously.[42] RNA-Seq libraries were constructed from 1 μg total RNA after rRNA depletion using Ribo-Zero GOLD (Illumina). The Illumina TruSeq RNA Sample Prep V2 Kit was used according to manufacturer's instructions except where noted. The data were processed using RTA v. 1.18.64 and CASAVA v. 1.8.2. The data for 23 PN and two normal adult Schwann cells samples were further processed using standard Tuxedo pipeline.[43] The resulting gene expression from transcriptome datasets were then log2 transformed and standardized (*z*-scored). Genes with the median log2 FPKM score below 0.5 in both groups (PN and normal Schwann cells) were considered unexpressed and removed from the analysis. The resulting expression set of 11 293 genes was analyzed with GSEA as described.[44] We used 5000 permutations and shuffled the expression dataset by gene-sets rather than by sample labels. Gene-sets with FDR < 0.01 were considered statistically significant and with $0.01 \leqslant \text{FDR} < 0.02$ as trending.

Copy number variation and loss of heterozygosity

CNV and LOH analyses were performed as described previously.[45] SNP genotyping was performed using HumanOmni2.5–8 BeadChip kits (Illumina) as per the manufacturer's instructions.

Non-*NF1* somatic mutation verification and deep *NF1* mutation detection by Ampliseq/IonTorrent

Multiplex PCR primers for somatic mutation verification were designed using the Ion Ampliseq Designer tool (v.3.0.1, Life Technologies, Grand Island, NY, USA). Multiplex PCR amplification, library preparation and sequencing on the Ion Proton sequencer (Life Technologies) were performed as per the manufacturer's instructions. Reads from the Ion Torrent Proton sequencer were filtered, and adapter- and quality-trimmed. The resulting sequences were aligned to human reference genome hg19 using TMAP (Life Technologies). Resulting BAM files were further aligned using The Genome Analysis Toolkit (GATK, http://www.nature.com/ng/journal/v43/n5/full/ng.806.html). For missense and nonsense mutations, *NF1* cDNA was examined by reverse-transcription PCR (Superscript II, Invitrogen) using primers flanking the affected exon, followed by Sanger sequencing (ABI Big Dye 3) to screen for splicing errors.

Whole exome sequencing analysis

The data were processed with two pipelines ('NISC' and 'Broad') (Supplementary Figure S1A) and somatic mutations were identified by subtracting germline variants. Alternatively, somatic variants were called by MuTect[46] (Broad pipeline; Supplementary Figure S1B). Potential causative genes were analyzed with driver-passenger software.[47] Select somatic mutations were verified by using AmpliSeq and IonTorrent sequencing of targeted PCR products. IonTorrent sequencing data were compared with WES data; mutations identified by both technologies in the same tumor samples were deemed 'high-confidence' variants. Given the importance of *NF1* in the tumors, we included the entire coding part of the gene into the AmpliSeq/IonTorrent validation effort. The NISC pipeline included the following components: Novoalign, v.2.08.02 (Novocraft.com, Selangor, Malaysia) for read alignment to hg19; duplicate removal with samtools;[48] bam2mpg for genotype calling and calculation of the quality score most probable genotype[49] and ANNOVAR for functional annotation of genetic variants[50] (http://www.openbioinformatics.org/annovar/). The resulting data were formatted in VarSifter[51] format (http://research.nhgri.nih.gov/software/VarSifter/) for further filtering. The filtering was done as follows. First, all non-coding variants and the nucleotides whose genotypes were identical in both tumor and corresponding normal DNA were removed. Second, from the remaining coding somatic variants all sequence variants that had a quality score (most probable genotype) < 10 either in tumor or normal DNA were removed.

The Broad pipeline included the following components: Burrows-Wheeler Aligner v. 0.6.2-r126[52] for mapping fastq files to hg19; Picard (https://broadinstitute.github.io/picard/) for removing duplicates; The Genome Analysis Toolkit (GATK) v.2.4–9[53] for local realignment and base quality recalibration; and GATK UnifiedGenotyper (https://software.broadinstitute.org/gatk/) for calling point mutations and insertions-deletions. ANNOVAR was used for functional annotation of genetic variants. Additional filtering used custom Perl scripts to remove all non-coding, low quality (score < 200) and common variants (1,000 Genomes and NHLBI Exome Sequencing Project variant frequency > 0.01) as well as variants with alternative allele frequency below 0.3. In addition, MuTect[46] was used to compare tumor with matched normal DNA and identify somatic point mutations.

In both pipelines, variants of interest were referenced against the Human Gene Mutation Database (HGMD: www.hgmd.cf.ac.uk), Exome Aggregation Consortium (ExAC: http://exac.broadinstitute.org/), and the Catalog of Somatic Mutations in Cancer, (COSMIC: http://cancer.sanger.ac.uk/cosmic).

Passenger/driver analysis

We used the Youn and Simon ('NCI_DPS') software developed at NCI[47] or MutSigCV (http://www.broadinstitute.org/cancer/cga/mutsig). The NCI software was used with both the NISC and Broad pipelines whereas MutSig was used only with the Broad pipeline. To prepare data for MutSigCV, predicted somatic mutations from the 23 PN were first converted to MAF

format using the UCSC 'known gene' annotations,[54] assigning an effect value of 'nonsilent' if a mutation altered the protein sequence for any of the annotated transcripts of a gene, 'silent' if the mutation resided within the coding sequence of a gene, and 'flank' if otherwise. Gene coverage, broken down by effect value, was evaluated similarly, making the assumption that a genomic position was 'covered' if both the tumor and the normal sample had adequate sequencing depth to genotype both samples with an most probable genotype score of 10 or greater.[49] For gene mutability covariate values, we used expression, replication time, and chromatin state values reported previously.[55] Coverage, MAF, and covariate files were then used as input to MutSigCV version 1.3.01[56] via the Broad Institute's GenePattern server.[57]

Allele-specific copy number and LOH analysis of PN

Paired CNV and LOH analysis of tumor and matching normal DNA was performed by using Nexus v.6.1 software (BioDiscovery Inc., Hawthorne, CA, USA) as described previously.[45] The analysis settings were selected based on the developer's suggestions for the analysis of tumor samples. 'Allele-Specific Copy number Analysis of Tumors' (ASCAT v.2.1) analysis was performed as previously described.[58]

The content of this publication does not necessarily reflect the views or policies of the Department of Health and Human Services, nor does mention of trade names, commercial products or organizations imply endorsement by the US Government.

CONFLICT OF INTEREST

The authors declare no conflict of interest.

ACKNOWLEDGEMENTS

Funding provided by the Intramural Research Programs of the National Human Genome Research Institute, the Center for Cancer Research of the National Cancer Institute and the Division of Cancer Epidemiology and Genetics of the National Cancer Institute. We thank the members of the NISC Comparative Sequencing Program: Betty Barnabas, PhD, Robert Blakesley, PhD, Gerry Bouffard, PhD, Shelise Brooks, BS, Holly Coleman, MSc, Mila Dekhtyar, MSc, Michael Gregory, MSc, Xiaobin Guan, PhD, Jyoti Gupta, MSc, Joel Han, BS, Shi-ling Ho, BS, Richelle Legaspi, MSc, Quino Maduro, BS, Cathy Masiello, MSc, Baishali Maskeri, PhD, Jenny McDowell, PhD, Casandra Montemayor, MSc, Morgan Park, PhD, Nancy Riebow, BS, Karen Schandler, MSc, Brian Schmidt, BS, Christina Sison, BS, Mal Stantripop, BS, James Thomas, PhD, Pam Thomas, PhD, Meg Vemulapalli, MSc, Alice Young, BA. We also thank the members of the NCI DCEG Cancer Genomics Research Laboratory: Michael Beerman, Aaron J Bouk, Seth Brodie, Laurie Burdett, Salma Chowdhury, Charles Chung, Nathan Cole, Michael Cullen, Casey Dagnall, Danielle Debacker, Sadie Frary, Chris Hautman, Belynda Hicks, Herb Higson, Keisha Hines-Harris, Amy Hutchinson, Kristie Jones, Eric Karlins, Sally Larson, Kerrie Lashley, Hyo Jung Lee, Shengchao Li, Tong Li, Wen Luo, Mike Malasky, Michelle Manning, Charles McCoy, Jason Mitchell, Adri O'Neil, Padma Ramya Packirisamy, Timothy Pelc, David Roberson, Aaron Rodriguez, Marianne Siler, Shalabh Suman, Kedest Teshome, Julio Tun, Sue Turner, Bill Utermahlen, Aurelie Vogt, Sarah Wagner, Mingyi Wang, Zhaoming Wang, Kathleen Wyatt, Qi Yang, Meredith Yeager, Sherry Yu, Xijun Zhang, Weiyin Zhou, Bin Zhu. MRW acknowledges funding from the Department of Defense (DAMD17-98-1-8609, DAMD17-00-1-0549), the National Institutes of Health (R29 NS31550), and the Children's Tumor Foundation supporting the development of the PN cultures over a 17-year span. Finally, we thank the patients who enlisted the help of their physicians to contribute tissues to research.

REFERENCES

1 Jett K, Friedman JM. Clinical and genetic aspects of neurofibromatosis 1. *Genet Med* 2010; **12**: 1–11.
2 Neurofibromatosis. Conference statement. National Institutes of Health Consensus Development Conference. *Arch Neurol* 1988; **45**: 575–578.
3 Huson SM, Harper PS, Compston DA. Von Recklinghausen neurofibromatosis. A clinical and population study in south-east Wales. *Brain* 1988; **111**(Pt 6): 1355–1381.
4 Mautner VF, Asuagbor FA, Dombi E, Funsterer C, Kluwe L, Wenzel R *et al.* Assessment of benign tumor burden by whole-body MRI in patients with neurofibromatosis 1. *Neuro Oncol* 2008; **10**: 593–598.
5 Evans DG, Baser ME, McGaughran J, Sharif S, Howard E, Moran A. Malignant peripheral nerve sheath tumours in neurofibromatosis 1. *J Med Genet* 2002; **39**: 311–314.
6 Uusitalo E, Rantanen M, Kallionpaa RA, Poyhonen M, Leppavirta J, Yla-Outinen H *et al.* Distinctive cancer associations in patients with neurofibromatosis type 1. *J Clin Oncol* 2016; **34**: 1978–1986.
7 Kim A, Gillespie A, Dombi E, Goodwin A, Goodspeed W, Fox E *et al.* Characteristics of children enrolled in treatment trials for NF1-related plexiform neurofibromas. *Neurology* 2009; **73**: 1273–1279.
8 Babovic-Vuksanovic D, Widemann BC, Dombi E, Gillespie A, Wolters PL, Toledo-Tamula MA *et al.* Phase I trial of pirfenidone in children with neurofibromatosis 1 and plexiform neurofibromas. *Pediatr Neurol* 2007; **36**: 293–300.
9 Widemann BC, Babovic-Vuksanovic D, Dombi E, Wolters PL, Goldman S, Martin S *et al.* Phase II trial of pirfenidone in children and young adults with neurofibromatosis type 1 and progressive plexiform neurofibromas. *Pediatr Blood Cancer* 2014; **61**: 1598–1602.
10 Weiss B, Widemann BC, Wolters P, Dombi E, Vinks AA, Cantor A *et al.* Sirolimus for non-progressive NF1-associated plexiform neurofibromas: an NF clinical trials consortium phase II study. *Pediatr Blood Cancer* 2014; **61**: 982–986.
11 Peltonen J, Jaakkola S, Lebwohl M, Renvall S, Risteli L, Virtanen I *et al.* Cellular differentiation and expression of matrix genes in type 1 neurofibromatosis. *Lab Invest* 1988; **59**: 760–771.
12 Stemmer-Rachamimov A, Nielsen GP. Pathologic and molecular diagnostic features of peripheral nerve sheath tumors in NF1. In: Upadhyaya M, Cooper DN (eds). *Neurofibromatosis Type 1: Molecular and Cellular Biology*. Springer: Heidlberg, 2012. pp 429–443.
13 Serra E, Rosenbaum T, Winner U, Aledo R, Ars E, Estivill X *et al.* Schwann cells harbor the somatic NF1 mutation in neurofibromas: evidence of two different Schwann cell subpopulations. *Hum Mol Genet* 2000; **9**: 3055–3064.
14 Maertens O, Brems H, Vandesompele J, De Raedt T, Heyns I, Rosenbaum T *et al.* Comprehensive NF1 screening on cultured Schwann cells from neurofibromas. *Hum Mutat* 2006; **27**: 1030–1040.
15 Sabbagh A, Pasmant E, Laurendeau I, Parfait B, Barbarot S, Guillot B *et al.* Unravelling the genetic basis of variable clinical expression in neurofibromatosis 1. *Hum Mol Genet* 2009; **18**: 2768–2778.
16 Castle B, Baser ME, Huson SM, Cooper DN, Upadhyaya M. Evaluation of genotype-phenotype correlations in neurofibromatosis type 1. *J Med Genet* 2003; **40**: e109.
17 Pasmant E, Sabbagh A, Masliah-Planchon J, Ortonne N, Laurendeau I, Melin L *et al.* Role of noncoding RNA ANRIL in genesis of plexiform neurofibromas in neurofibromatosis type 1. *J Natl Cancer Inst* 2011; **103**: 1713–1722.
18 Beert E, Brems H, Daniels B, De Wever I, Van Calenbergh F, Schoenaers J *et al.* Atypical neurofibromas in neurofibromatosis type 1 are premalignant tumors. *Genes Chrom Cancer* 2011; **50**: 1021–1032.
19 Luscan A, Shackleford G, Masliah-Planchon J, Laurendeau I, Ortonne N, Varin J *et al.* The activation of the WNT signaling pathway is a Hallmark in neurofibromatosis type 1 tumorigenesis. *Clin Cancer Res* 2014; **20**: 358–371.
20 Zhang M, Wang Y, Jones S, Sausen M, McMahon K, Sharma R *et al.* Somatic mutations of SUZ12 in malignant peripheral nerve sheath tumors. *Nat Genet* 2014; **46**: 1170–1172.
21 Lee W, Teckie S, Wiesner T, Ran L, Prieto Granada CN, Lin M *et al.* PRC2 is recurrently inactivated through EED or SUZ12 loss in malignant peripheral nerve sheath tumors. *Nat Genet* 2014; **46**: 1227–1232.
22 Hirbe AC, Dahiya S, Miller CA, Li T, Fulton RS, Zhang X *et al.* Whole exome sequencing reveals the order of genetic changes during malignant transformation and metastasis in a single patient with NF1-plexiform neurofibroma. *Clin Cancer Res* 2015; **21**: 4201–4211.
23 Kircher M, Witten DM, Jain P, O'Roak BJ, Cooper GM, Shendure J. A general framework for estimating the relative pathogenicity of human genetic variants. *Nat Genet* 2014; **46**: 310–315.
24 Colman SD, Williams CA, Wallace MR. Benign neurofibromas in type 1 neurofibromatosis (NF1) show somatic deletions of the NF1 gene. *Nat Genet* 1995; **11**: 90–92.
25 Kannan K, Inagaki A, Silber J, Gorovets D, Zhang J, Kastenhuber ER *et al.* Whole-exome sequencing identifies ATRX mutation as a key molecular determinant in lower-grade glioma. *Oncotarget* 2012; **3**: 1194–1203.
26 Barretina J, Taylor BS, Banerji S, Ramos AH, Lagos-Quintana M, Decarolis PL *et al.* Subtype-specific genomic alterations define new targets for soft-tissue sarcoma therapy. *Nat Genet* 2010; **42**: 715–721.
27 Parsons DW, Jones S, Zhang X, Lin JC, Leary RJ, Angenendt P *et al.* An integrated genomic analysis of human glioblastoma multiforme. *Science* 2008; **321**: 1807–1812.
28 Wu G, Broniscer A, McEachron TA, Lu C, Paugh BS, Becksfort J *et al.* Somatic histone H3 alterations in pediatric diffuse intrinsic pontine gliomas and non-brainstem glioblastomas. *Nat Genet* 2012; **44**: 251–253.
29 Le LQ, Liu C, Shipman T, Chen Z, Suter U, Parada LF. Susceptible stages in Schwann cells for NF1-associated plexiform neurofibroma development. *Cancer Res* 2011; **71**: 4686–4695.

30 Buchstaller J, Clapp DW, Parada LF, Zhu Y. Cell of Origin and the Contribution of Microenvironment in NF1 Tumorigenesis and Therapeutic Implications. In: Upadhyaya M, Cooper DN (eds). *Neurofibromatosis Type 1: Molecular and Cellular Biology*. Springer: Heidelberg, 2012.

31 Wallace MR, Rasmussen SA, Lim IT, Gray BA, Zori RT, Muir D. Culture of cytogenetically abnormal schwann cells from benign and malignant NF1 tumors. *Genes Chromosomes Cancer* 2000; **27**: 117–123.

32 Laycock-van Spyk S, Thomas N, Cooper DN, Upadhyaya M. Neurofibromatosis type 1-associated tumours: their somatic mutational spectrum and pathogenesis. *Hum Genomics* 2011; **5**: 623–690.

33 Upadhyaya M, Spurlock G, Monem B, Thomas N, Friedrich RE, Kluwe L *et al.* Germline and somatic NF1 gene mutations in plexiform neurofibromas. *Hum Mutat* 2008; **29**: E103–E111.

34 Emi M, Matsushima M, Katagiri T, Yoshimoto M, Kasumi F, Yokota T *et al.* Multiplex mutation screening of the BRCA1 gene in 1000 Japanese breast cancers. *Jpn J Cancer Res* 1998; **89**: 12–16.

35 Dode C, Levilliers J, Dupont JM, De Paepe A, Le Du N, Soussi-Yanicostas N *et al.* Loss-of-function mutations in FGFR1 cause autosomal dominant Kallmann syndrome. *Nat Genet* 2003; **33**: 463–465.

36 Levy P, Ripoche H, Laurendeau I, Lazar V, Ortonne N, Parfait B *et al.* Microarray-based identification of tenascin C and tenascin XB, genes possibly involved in tumorigenesis associated with neurofibromatosis type 1. *Clin Cancer Res* 2007; **13**: 398–407.

37 Pasmant E, Ortonne N, Rittie L, Laurendeau I, Levy P, Lazar V *et al.* Differential expression of CCN1/CYR61, CCN3/NOV, CCN4/WISP1, and CCN5/WISP2 in neurofibromatosis type 1 tumorigenesis. *J Neuropathol Exp Neurol* 2010; **69**: 60–69.

38 Miller SJ, Jessen WJ, Mehta T, Hardiman A, Sites E, Kaiser S *et al.* Integrative genomic analyses of neurofibromatosis tumours identify SOX9 as a biomarker and survival gene. *EMBO Mol Med* 2009; **1**: 236–248.

39 Smithson LJ, Anastasaki C, Chen R, Toonen JA, Williams SB, Gutmann DH. Contextual signaling in cancer. *Semin Cell Dev Biol* 2016; **58**: 118–126.

40 Upadhyaya M, Spurlock G, Thomas L, Thomas NS, Richards M, Mautner VF *et al.* Microarray-based copy number analysis of neurofibromatosis type-1 (NF1)-associated malignant peripheral nerve sheath tumors reveals a role for Rho-GTPase pathway genes in NF1 tumorigenesis. *Hum Mutat* 2012; **33**: 763–776.

41 Muir D, Neubauer D, Lim IT, Yachnis AT, Wallace MR. Tumorigenic properties of neurofibromin-deficient neurofibroma Schwann cells. *Am J Pathol* 2001; **158**: 501–513.

42 Pemov A, Sung H, Hyland PL, Sloan JL, Ruppert SL, Baldwin AM *et al.* Genetic modifiers of neurofibromatosis Type 1-Associated Cafe-au-Lait macule count identified using multi-platform analysis. *PLOS Genet* 2014; **10**: e1004575.

43 Trapnell C, Roberts A, Goff L, Pertea G, Kim D, Kelley DR *et al.* Differential gene and transcript expression analysis of RNA-seq experiments with TopHat and Cufflinks. *Nat Protoc* 2012; **7**: 562–578.

44 Subramanian A, Tamayo P, Mootha VK, Mukherjee S, Ebert BL, Gillette MA *et al.* Gene set enrichment analysis: a knowledge-based approach for interpreting genome-wide expression profiles. *Proc Natl Acad Sci USA* 2005; **102**: 15545–15550.

45 Dewan R, Pemov A, Kim HJ, Butman JA, Morgan K, Vasquez RA *et al.* Evidence of multiple independent tumor initiation events in neurofibromatosis type 2-associated vestibular schwannomas. *Neuro Oncol* 2014; **17**: 566–573.

46 Cibulskis K, Lawrence MS, Carter SL, Sivachenko A, Jaffe D, Sougnez C *et al.* Sensitive detection of somatic point mutations in impure and heterogeneous cancer samples. *Nat Biotechnol* 2013; **31**: 213–219.

47 Youn A, Simon R. Identifying cancer driver genes in tumor genome sequencing studies. *Bioinformatics* 2011; **27**: 175–181.

48 Li H, Handsaker B, Wysoker A, Fennell T, Ruan J, Homer N *et al.* The Sequence Alignment/Map format and SAMtools. *Bioinformatics* 2009; **25**: 2078–2079.

49 Teer JK, Bonnycastle LL, Chines PS, Hansen NF, Aoyama N, Swift AJ *et al.* Systematic comparison of three genomic enrichment methods for massively parallel DNA sequencing. *Genome Res* 2010; **20**: 1420–1431.

50 Wang K, Li M, Hakonarson H. ANNOVAR: functional annotation of genetic variants from high-throughput sequencing data. *Nucleic Acids Res* 2010; **38**: e164.

51 Teer JK, Green ED, Mullikin JC, Biesecker LG. VarSifter: visualizing and analyzing exome-scale sequence variation data on a desktop computer. *Bioinformatics* 2012; **28**: 599–600.

52 Li H, Durbin R. Fast and accurate short read alignment with Burrows-Wheeler transform. *Bioinformatics* 2009; **25**: 1754–1760.

53 DePristo MA, Banks E, Poplin R, Garimella KV, Maguire JR, Hartl C *et al.* A framework for variation discovery and genotyping using next-generation DNA sequencing data. *Nat Genet* 2011; **43**: 491–498.

54 Hsu F, Kent WJ, Clawson H, Kuhn RM, Diekhans M, Haussler D. The UCSC known genes. *Bioinformatics* 2006; **22**: 1036–1046.

55 Cancer Genome Atlas Research N, Comprehensive genomic characterization of squamous cell lung cancers. *Nature* 2012; **489**: 519–525.

56 Lawrence MS, Stojanov P, Polak P, Kryukov GV, Cibulskis K, Sivachenko A *et al.* Mutational heterogeneity in cancer and the search for new cancer-associated genes. *Nature* 2013; **499**: 214–218.

57 Reich M, Liefeld T, Gould J, Lerner J, Tamayo P, Mesirov JP. GenePattern 2.0. *Nat Genet* 2006; **38**: 500–501.

58 Van Loo P, Nilsen G, Nordgard SH, Vollan HK, Borresen-Dale AL, Kristensen VN *et al.* Analyzing cancer samples with SNP arrays. *Methods Mol Biol* 2012; **802**: 57–72.

Supplementary Information accompanies this paper on the Oncogene website (http://www.nature.com/onc)